

Supplementary Information

Generation of highly luminescent micro rings by optical irradiation

Jiwoong Kwon,^{§†a} Doyk Hwang,^{†a} Jong Woo Lee,^b Inhae Zoh,^a

Jooyoun Kang^b and Seong Keun Kim^{*a,b}

^a Department of Biophysics and Chemical Biology, Seoul National University, Seoul 08826, Republic of Korea.

^b Department of Chemistry, Seoul National University, Seoul 08826, Republic of Korea.

[§] Current Address: Center for Molecular Spectroscopy and Dynamics, Institute for Basic Science, Seoul 02841,

Republic of Korea; Department of Chemistry, Korea University, Seoul 02841, Republic of Korea.

[†] These authors equally contributed to this work.

^{*} Correspondence and requests for materials should be addressed to S. K. K. (seongkim@snu.ac.kr)

Experimental Details

Optical microscopy and spectroscopy

All optical experiments were performed using a home-built microscope (Fig. S1). Two laser beams (532 nm: SambaTM 532, Cobolt; 633 nm: 25-LHP-928-230, CVI Melles-Griot) were combined into a single optical path with dichroic mirrors (ZT532rdc, Chroma), and coupled to a single-mode fiber ($\Phi = 4.2 \mu\text{m}$, P1-630PM-FC, Thorlabs) to make Gaussian-like beams. They passed through a second dichroic mirror (ZT375/488/532/633rpc, Chroma) which removed scattered light from luminescence signals. An achromatic $\lambda/4$ retarder (RAC-3.4.15, Bernhard Halle Nachfl.) was employed to make the circularly polarized excitation light for efficient excitation of the sample. An oil-immersion objective lens (UIS2 series, PlanApo N, NA = 1.4, 100x, Olympus) effectively focuses the excitation light and collect the transmitted, scattered and luminescence signals. The sample was placed on a piezo stage (Nanomax Max311, Thorlabs) that can precisely scan the sample for scanning-based luminescence/scattering imaging. A common white light LED placed above the sample stage was also used as an illumination light source for bright-field imaging.

A removable pellicle beam splitter (BP145B1, Thorlabs) was introduced for the bright-field and scattering images to avoid severe signal loss due to the dichroic mirrors, whereas the luminescence signals were collected after passing the dichroic mirrors without the pellicle beam splitter. Three photodetectors, which were selectable by using flip mirrors, were employed to acquire the signals: an avalanche photodiode (APD, SPCM-AQR-14FC, Perkin Elmer) coupled to a multi-mode fiber ($\Phi = 62.5 \mu\text{m}$, M31L02, Thorlabs) acts as a pinhole in the confocal luminescence imaging mode; A photomultiplier tube (MP962, Perkin Elmer) with active quenching control collects scattered signals without the pinhole to generate scattering images; a WebCam (VX1000, Microsoft) with a relatively low detection quantum yield records signals when extremely large photon counts are expected as in the case of taking a movie for the LMR formation. The detection lenses that effectively focus optical signals to the detectors were selected by considering the size of the confocal pinhole or wide-field image magnification. If an emission filter was needed to separate the signals from backgrounds, a proper filter was placed in front of each detector (Table S1). The acquired signals were analyzed by a multi-channel scaler (P7882, Fast ComTech) or a data acquisition board provided by the supplier and then processed by the imaging software also provided by the supplier, except when the Inspector program provided by the Prof. Stefan W. Hell group of Germany was used for scanning-based imaging.

In order to characterize the emission spectra from dye solutions, solid powders and the LMR, a portable spectrometer (SM240, Spectral Products) replaced the APD (Table S1). For the lifetime analysis, light from a femtosecond laser (MaiTai, Spectra-physics) with supercontinuum generator (FemtoWHITE-800, NKT Photonics) and appropriate bandpass filter excited the sample (Table S1), and a time-correlated single photon counter (SPC-150, Becker & Hickl GmbH) analyzed the collected photons to generate luminescence decay profiles. The height/phase imaging of the LMR was performed using a commercially available atomic force microscope system (NanoWizard, JPK Instruments).

Sample preparation

Since almost all of experiments were performed on the optical microscope, the sample was basically prepared on the microscope cover glass (0101242, Marienfeld). We used plastic coverslips (12547, Fisher Scientific) as a different substrate. Depending on the type of light absorbing molecules, we prepared each sample in the following conditions.

1. [Liquid samples containing dye molecules] We made 2 mM aqueous solutions of fluorescein (F6377, Sigma Aldrich), rhodamine 6G (R6G, 83697, Sigma Aldrich) and methylene blue (M9140, Sigma Aldrich). To test the importance of absorbance of samples, we prepared 50 mM solution of phenolphthalein (PhP, 015945, Sigma Aldrich) in EtOH (A995-4, Fisher Scientific) and used 1 M aqueous solution of NaOH (7571-4400, Daejung Chemicals & Metals) to make the basic PhP sample (PhP in EtOH : NaOH(aq) = 98 : 2, volume ratio). Effect of sample's charges/ions were tested by using [2 mM R6G + 20 mM NaCl] aqueous solution and 2 mM Nile Red (N0659, TCI) solution in methoxybenzene (A0492, TCI). A 2 mM Atto540Q (AD540Q-21, Atto-tec) solution in acetonitrile (9017-03, J.T.Baker) was used as a nonfluorescent but highly absorbing sample. In order to remove aggregated particles and impurities, the samples were mildly sonicated for more than 60 minutes and filtered by a syringe filter with a 20-nm pore size (6809-1102, Whatman GmbH). A small volume (~20 µL) of sample was dropped onto the cover glass for further experiments.
2. [Surface-bound nanoparticles] We tested three kinds of nanoparticles: 30, 35, 50, 100 and 140 nm fluorescent nanodiamonds (FND) from the Dr. Huan-Cheng Chang group of Taiwan, 80 nm gold colloid (EM.GC80, BBI Solutions) and CdSe/ZnS quantum dot (Q21321MP, Invitrogen). All nanoparticles were immobilized on the surface of the cover glass through the electrostatic interaction, resulted from treatment of the cover glass with poly-L-lysine solution (P8920, Sigma Aldrich) for 3 minutes to coat the surface with positive charges. After washing out the poly-L-lysine with deionized water, the aqueous solutions of nanoparticles were incubated on the surface for 3 minutes to induce electrostatic binding to the surface. The unbound nanoparticles were washed out with deionized water, and finally a proper mounting medium was applied on the cover glass.
3. [Transparent polymer matrices] PDMS elastomer (SYLGARD® 184, Dow Corning) and PMMA (MW ~15,000 and 350,000, Sigma Aldrich) were used as model systems for transparent polymer matrices. PDMS was coated on the glass surface following the protocol provided by the company. PMMA was dissolved in a chloroform solvent and the solution was drop-casted on the glass surface. The glass coverslip was then baked in an oven at 80 °C for 30 minutes to remove the solvent and obtain the glass surface coated with PMMA.
4. [Dye powder] In our fluorescence lifetime measurement of R6G powder for comparison with those of R6G solution and the LMR, the sample powder was dropped on the glass surface and used without further treatment.

When we characterized the LMR, the mounting media was removed by vigorous washing of the glass coverslip with acetone, methanol, and deionized Milli-Q water. The LMR strongly adhered to the glass surface, even sonication in various solvents cannot remove it from glass coverslips. All images and spectra in Figs. 1, 2, and 3 were obtained without any mounting medium. If long-term generation and observation of the LMR was necessary in the liquid medium, we used a cover glass bottom dish (100350, SPL Life Sciences) as a sample container to reduce the effect of solvent evaporation. In particular, when we tested benzene and other aromatic hydrocarbons, we used a homemade sample container made of stainless steel to avoid unintended generation of organic impurities resulting from dissolution of container materials into the solvent.

Supplementary Movie S1 Real-time observation of the formation process of the LMR was recorded using a WebCam for a 2 mM aqueous solution of R6G under 7 mW laser irradiation at 532 nm. We placed an emission bandpass filter (ET700/75m, Chroma) in front of the WebCam to reduce the strong fluorescence signal from R6G and the scattered light. A white light LED was used for the wide-field illumination and the transmitted photons were detected for imaging. When we used a high power of the excitation laser, we immediately observed a dynamic motion of the bright spot (at ~4 seconds), which may represent solvent evaporation. At a certain time (~8 seconds) during irradiation, a ‘burst’ took place and the LMR seemed to be formed at the time. After the ‘burst’, solvent evaporation took place again, in an asymmetric way, which appeared as a dark arc in the movie (at 10~50 seconds). After sufficient irradiation, the dynamic process seemed to end with no further change. When the excitation laser was turned off, the LMR was clearly visible at the irradiation center (after 60 seconds).

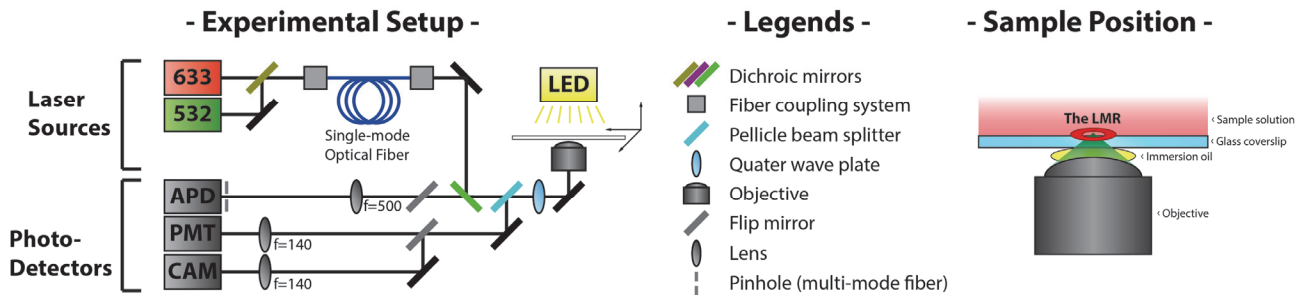


Figure S1 A schematic design for the home-built optical microscope. A white light LED and three lasers were used as the light source for optical imaging. A quarter waveplate made the excitation light circularly polarized. The sample was placed on a piezo stage for precise control of scanning. In order to avoid severe signal loss, a pellicle beam splitter was introduced to split the scattered light to another beam path that cannot pass through the dichroic mirror. A WebCam that has strong resistance against photo-damage was used for bright field imaging and taking the movie of the LMR formation (Supplementary Movie S1). Scanning-based luminescence and scattering images were obtained by the APD and PMT.

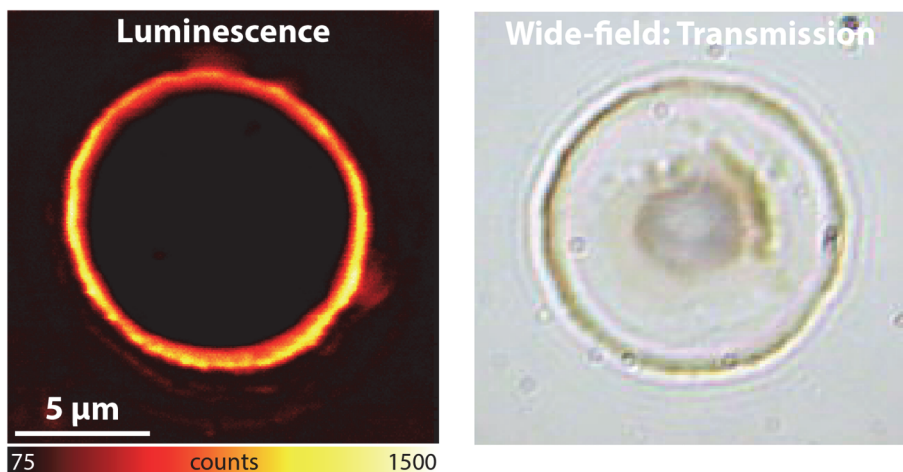


Figure S2 Comparison of the confocal luminescence image (Left) and wide-field transmission image (Right) of the LMR shown in Fig. 1. The LMR showed poor efficiency for transmission as well as scattering. The length scale of the wide-field transmission image did not exactly follow the scale bar, but was roughly adjusted.

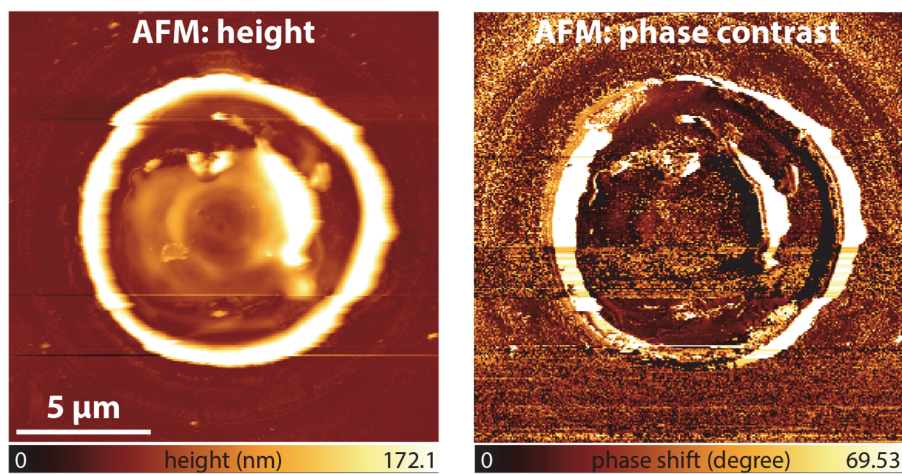


Figure S3 Comparison of the surface morphology (Left) and phase contrast image (Right) of the LMR shown in Fig. 1. The LMR and additional structures inside the ring form protruded microstructures with a height of >100 nm. The lock-in phase shift of these microstructures was larger than that of the glass surface, suggesting that the LMR is composed of softer materials than the glass.

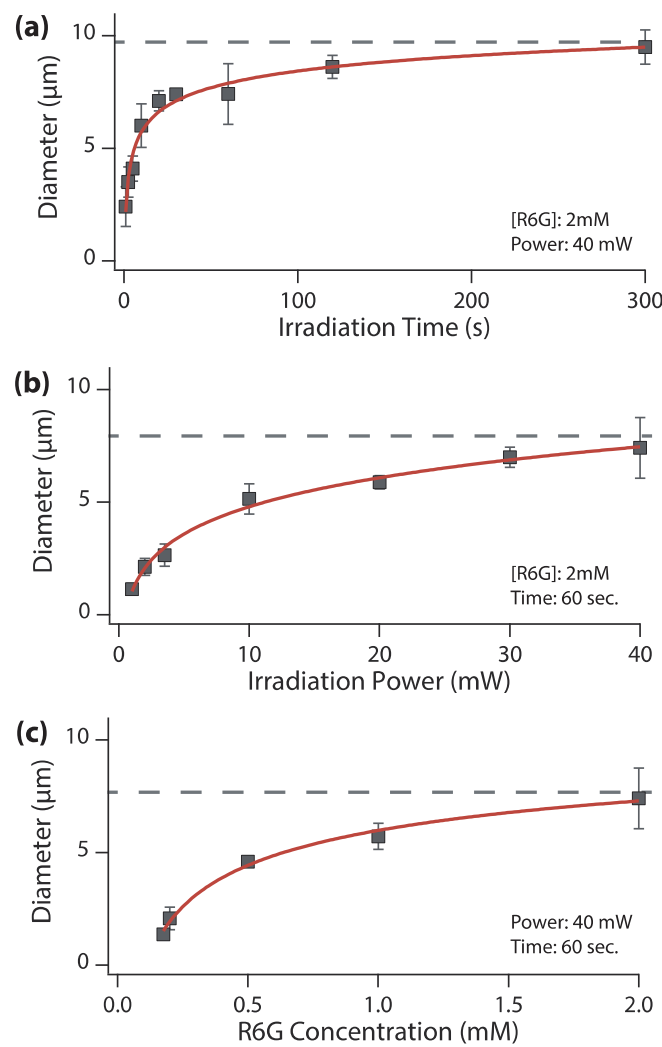


Figure S4 Change in the diameter of the LMR as a function of (a) irradiation time, (b) irradiation power, and (c) the concentration of absorbing molecule (R6G). Red lines are guides for the eye, not fitted lines. The grey dashed-lines indicate possible saturation values.

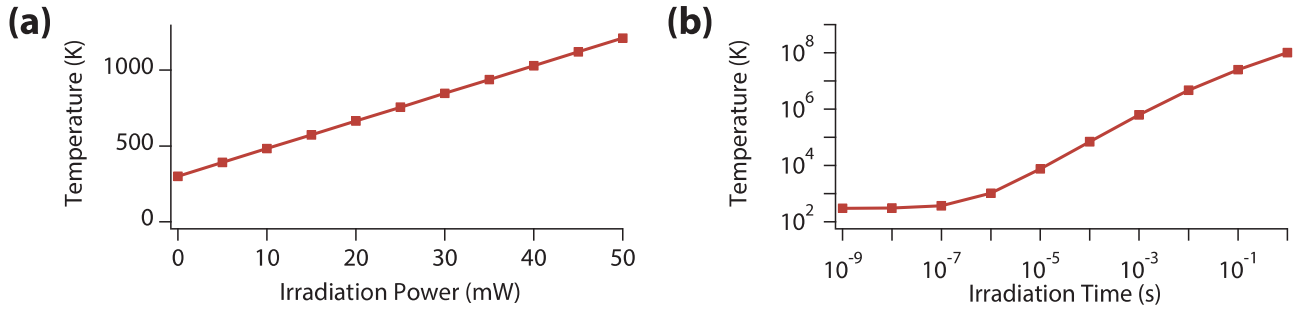


Figure S5 Simulated temperature at the interface between the glass coverslip and the light-absorbing medium (a 2mM aqueous solution of R6G) as a function of (a) the irradiation power (at 1 μ s) and (b) the irradiation time (at 40 mW) [K. Zimmer, *Intl. J. Heat Mass Transfer*, 2009, **52**, 497.]. Irradiation beam size for the simulation is 600 nm in diameter, typical value in confocal microscope with high-NA objective lens. Convection, radiation, and phase transitions were neglected in this simulation. Without these heat transport processes that lower the interfacial temperature, it reaches a sufficiently high temperature after \sim 1 μ s (when using 40 mW of laser power) to evaporate water-based media and to initiate thermal reactions. In reality, interfacial cooling will happen quite efficiently but nevertheless, a local region with a sufficiently high temperature may still be present for the above processes.

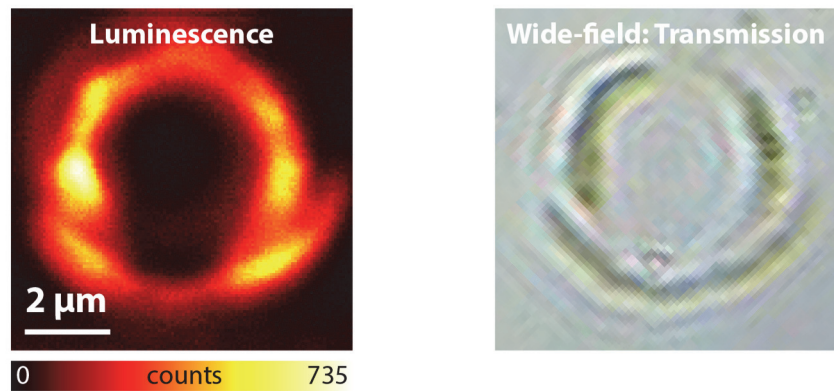


Figure S6 Comparison of the confocal luminescence image (Left) and wide-field transmission image (Right) of the LMR generated with 2 mM Atto540Q solution in acetonitrile. The LMR showed bright luminescence despite the very low fluorescence quantum yield of the quencher dye Atto540Q. The length scale of the wide-field transmission image does not exactly follow the scale bar but is roughly adjusted.

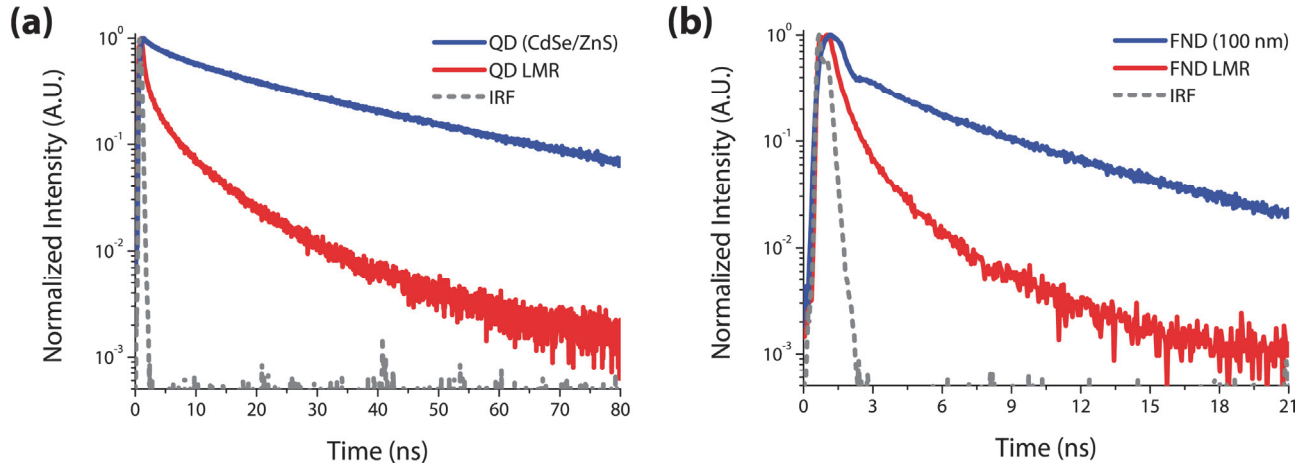


Figure S7 Comparison of the TCSPC photoluminescence lifetimes of nanoparticle absorbers QD and FND vs. those of the LMRs generated from them in immersion oil (manufactured by Olympus, containing 1,3,5-triisopropylbenzene as a major component). In both cases, the LMR exhibits a much shorter lifetime and more complex decay profile, which suggests that the LMR may contain complex materials resulting from diverse photothermal processes.

| | Luminescence | Transmission | Scattering | Spectrum | Lifetime |
|------------------------|---------------------|---------------------|-------------------|-----------------|----------------------------|
| Light Source | CW 532 nm | White light LED | CW 532 nm | CW 532 nm | Femtosecond Ti:sapphire |
| Emission Filter | LP03-532RE-25 | - | ET525/50m | LP03-532RE-25 | LP03-532RE-25 |

Table S1 Light sources and emission filters used in each experiment. In particular, we changed the dichroic mirror that reflects the excitation light and transmits the luminescence (ZT375/488/532/633rpc → ZT532rdc, not shown in table) to prevent the spectral deformation due to the dichroic mirror while getting photoluminescence spectrum of the LMR.